# Block Copolymer Micelles for Nucleation of Microcellular Thermoplastic Foams

**Pieter Spitael, Christopher W. Macosko,* and Richard B. McClurg***

*Department of Chemical Engineering and Materials Science, 421 Washington Ave. SE., University of Minnesota, Minneapolis, Minnesota 55455*

*Received February 11, 2004; Revised Manuscript Received June 1, 2004*

ABSTRACT: The use of block copolymer micelles as novel nucleating agents for foaming thermoplastics is explored. Diblock copolymers can self-assemble into a large number of spherical micelles, making them promising nucleants for the production of microcellular foams with $>10^9$ cells/cm$^3$. Different types of A−B diblock copolymers were added to a polystyrene matrix in low concentrations, and the resulting blends were foamed in a batch process using carbon dioxide as the blowing agent. Polystyrene-*b*-poly(ethylene propylene) and polystyrene-*b*-poly(methyl methacrylate) diblocks were not effective as nucleants. Diblocks containing poly(dimethylsiloxane) as the core block showed a bimodal cell size distribution and a small increase in cell concentration. The increased solubility of carbon dioxide in poly(dimethylsiloxane) (PDMS), and the reduced surface tension of PDMS, lowered the minimum work of bubble formation and increased the cell concentration. None of the foams showed an increase in cell concentration proportional to the large number of potential nucleants present. Block copolymer micelles as nucleants were not able to sufficiently lower the work of formation for cell nucleation. They are too small in size, can still agglomerate into larger, nonequilibrium structures, and have large contact angles due to the high surface tension of most polymers.

## Introduction

New applications for foamed materials and the ability to foam a wider variety of plastic materials will push their US consumption to a projected 7.8 billion pounds in 2005.[1] Almost half of this demand stems from polystyrene (PS), poly(vinyl chloride) (PVC), and other thermoplastic foams. Despite their significant success, continued growth of foamed polymers into new markets depends on the ability to enhance control over the cellular structure. The number and size of cells have a significant effect on the mechanical properties and ultimately the applications for thermoplastic foams.[2,3] Conventional thermoplastic foam processing methods result in a broad cell size distribution with cell concentrations lower than $10^6$ cells/cm$^3$ and an average cell size greater than 300 $\mu$m.[4] These large, nonuniform cells lead to a deterioration of the mechanical properties of the final product. Smaller and more uniform cells can improve mechanical properties and allows for the production of thinner parts while maintaining the physical integrity of the material.

Foams with cell sizes of 30 $\mu$m or less at high concentrations are classified as microcellular foams.[5] These foams were originally invented to reduce material consumption in mass-produced plastic parts without significant penalties in mechanical properties through the introduction of a large number of extremely small cells. Microcellular polymers have shown improved fatigue life and energy absorption,[6−8] increased toughness,[9,10] high thermal stability,[11] and good insulating properties.[3] The microcellular foam process can also reduce production cost and improve processing efficiency by allowing for reduced cycle times and faster demolding of thick parts in injection molding applications.[12] The process typically requires higher nucleation rates and higher inert gas concentrations than conventional processes.[13]

As early as the 1960s, Hansen and Martin showed the use of nucleating agents to aid in foam nucleation.[14,15] Several experimental and theoretical studies have been performed since then on the effect of nucleating agents in the processing of thermoplastic foams.[16−25] Inorganic particles such as talc, silicon oxide, titanium oxide, diatomaceous earth, and kaolin are among the most commonly used nucleants.[3] They are generally micron-sized but can be prone to agglomeration. Yang and Han[22] studied nine different nucleating agents, but only a trial-and-error process is outlined for selecting an appropriate nucleating agent. While the use of a variety of nucleating agents to give some control over the number of cells initially formed is well established, a clear understanding of their effect is lacking. More importantly, traditional nucleating agents are too large, and prone to agglomeration, to be suitable for the processing of microcellular materials where the final cell size ideally is less than 1 $\mu$m.

We investigate the use of block copolymer micelles as heterogeneous nucleation agents. Our goal is to increase the cell concentration, decrease the cell size, and widen the processing conditions under which a microcellular material may be obtained. Small, uniformly distributed block copolymer micelles have several of the desired requirements to form a favorable nucleation site.[26] This is believed to be the first use of micelles as heterogeneous nucleation sites for foam formation. Block copolymers have been reported as components in foam formulations,[27−29] but no details as to their role in the foam nucleation process are offered. Here we present a systematic study of three different block copolymers, as well as two solid nucleation agents, in an attempt to understand how the type and size of a nucleation site affects the thermoplastic foaming process. Before we present our experimental results, we describe ideal

* To whom correspondence should be addressed.

10.1021/ma049712q CCC: $27.50 
Published on Web 08/14/2004

nucleants and how block copolymer micelles could act as nucleants.

### Ideal Nucleants

Nucleating agents, or nucleants, are added to a polymer matrix to influence the bubble number density and/or size distribution in the final foam. The goal is to provide a controlled number and spatial distribution of sites that promote heterogeneous nucleation in a brief period of time so that the bubbles grow in tandem to a uniform size. The interplay between nucleation, whose rate is very sensitive to the blowing agent concentration, and bubble growth, which locally depresses the blowing agent concentration, determines the number density and size distribution of bubbles in the final foam. Ideal nucleants have four qualities that contribute to the desired behavior.[26]

- Nucleation on ideal nucleants is energetically favorable relative to homogeneous nucleation and heterogeneous nucleation on other additives and/or contaminants in the polymer matrix. Favorable energetics are found for surfaces with weak interactions with the polymer matrix and for radii of curvature that are large relative to the radius of the critical nucleus.[30,31]
- Ideal nucleants have uniform size and surface properties. If the nucleant population contains a distribution of sizes and/or surface properties, then they will activate over a wider time interval than if they had been uniform. In particular, a few easily activated nucleants can lead to a skewed or bimodal bubble size distribution in the foam.
- Ideal nucleants are easily dispersible. Aggregated nucleants are less efficient than dispersed ones since the first nucleant to activate in an aggregate depletes the blowing agent near the others.
- Ideal nucleants are plentiful. If there are insufficient nucleants, nucleation at unintended nucleation sites and homogeneous nucleation can be significant before the supersaturation is depressed by the growth of the bubbles resulting from nucleant activation. The result of insufficient nucleants is a skewed or bimodal bubble size distribution as a result of parallel nucleation mechanisms.

### Block Copolymer Micelles

Block copolymer micelles are potentially favorable nucleants adhering to the above qualifications. Spherical domains called micelles form when small amounts of a diblock copolymer are added to a homopolymer melt.[32−34] Diblock copolymers consist of two distinct polymers A and B covalently coupled together. When added to homopolymer A, for instance, the B chains of the diblock copolymers aggregate together in spherical domains to avoid unfavorable interactions with the A homopolymer. Typical micelles have a diameter on the order of tens of nanometers, dictated by the length and type of diblock copolymer.

The size and number of micelles present can be determined via several techniques. A direct observation can be made via transmission electron microscopy (TEM). An upper bound on the number of micelles ($n_m$) can then be established by assuming all of the copolymer resides in micelles:

$$n_m = \frac{wN_{av}}{M_n N_c} \tag{1}$$

where $w$ is the amount of diblock present, $N_{av}$ is Avogadro's number of chains/mol, and $M_n$ is the molecular weight of the diblock. $N_c$ is the number of copolymers per micelle, also known as the aggregation number, and is estimated independently.[35]

Alternatively, theoretical expressions exist that can give an estimate of the size and number of micelles present in block copolymer/homopolymer systems. Whitmore and Smith[35] present such a theory based on minimizing the free energy of the micellar system. They present the following expressions for core radius $l_b$, number density of micelles $n_m$, and number of copolymers per micelle $N_c$:

$$l_b = \left(\frac{\chi}{6}\right)^{1/6}\left(\frac{\rho_0}{\rho_{0B}}\right)^{1/3} Z_{cB}^{2/3} b \tag{2}$$

$$n_m = \left(\frac{27}{8\pi^2\chi}\right)^{1/2}\left(\frac{\rho_{0B}}{\rho_0 b^3}\right)\frac{\phi_{cB}^{2/3}}{Z_{cB}^{2}} \tag{3}$$

$$N_c = \left(\frac{8\pi^2\chi}{27}\right)^{1/2}(\rho_0 b^3) Z_{cB} \tag{4}$$

where $\chi$ is the polymer−polymer interaction parameter, $\rho_0$ is the geometric mean of the monomer number densities $\rho_{0A}$ and $\rho_{0B}$, $Z_{cB}$ is the degree of polymerization of polymer B, $b$ is an average Kuhn length, and $\phi_{cB}$ represents the overall volume fraction of B due to the block copolymer. These parameters are readily obtained from tabulated data.[36−38]

The cellular structure of foams results from the formation of bubbles through a nucleation process. There is a unique radius such that a bubble is in both chemical and mechanical equilibrium with its surroundings. J. W. Gibbs first introduced the concept of this critical nucleus and gives its value as[39]

$$r^* = \frac{2\sigma}{\Delta P} \tag{5}$$

Using a value of 34.5 mN/m for the surface tension ($\sigma$) of polystyrene[40] and a saturation pressure ($\Delta P$) of 3.5 MPa, we estimate a critical nucleus radius of 20 nm for our system. The radius of curvature of a micelle is comparable to this critical nucleus size. Even at low concentrations of block copolymer, the number density of micelles can easily exceed the number of cells observed in homogeneous nucleation. Block copolymer micelles are of the appropriate size for nucleation and exist in high concentrations and therefore could form a favorable nucleant.

### Experimental Section

We followed the batch process first outlined by Suh and coworkers in 1984.[41] Their process consists of three distinct steps. First, the polymer is saturated with a blowing agent in a pressure vessel at ambient temperature, then the pressure is released, and the sample is heated to produce a supersaturated sample. Density fluctuations in this metastable sample induce the nucleation of a large number of bubbles. Growth and possible coalescence of the nucleated cells leads to the final foam structure.

The matrix material for the blends described in this work is Styron 685D polystyrene with a weight-average molecular weight of 315 000 g/mol (The Dow Chemical Co.). The manufacturer reports that this polymer has no additives that could interfere with the nucleation behavior. Block copolymer is added to the polystyrene by melt-blending in a batch mixer

(Thermo-Haake Instruments, System 90) at various weight percentages from $^1/_2$ to 4%. Materials are mixed using roller blades in a 25*g* chamber at 200 °C. The mixer is operated at 35 rpm for the first 2 min as components are added and then increased to 75 rpm for an additional 5 min of mixing. The material is then pressed into circular disks (~1 g) at 200 °C using a hydraulic press. The samples are brought to temperature for 5 min, pressed at a low pressure (130 kPa) for 2 min, and pressed at a high pressure (900 kPa) for 8 min. They are then quenched to room temperature in approximately 3 min using cooling water. The disks have a final thickness of 2 mm and a diameter of 25 mm.

A small 300 mL pressure vessel (Parr Instrument Co., model 4760Q) is used to saturate the samples at room temperature with carbon dioxide gas. A minimum of 20 h was allowed to ensure uniform saturation for polystyrene samples. Finally, the samples are depressurized over 15 s and submerged in a silicon oil bath maintained at the desired foaming temperature. After the desired foaming time, samples are removed from the oil bath and quenched in ice water. All samples are foamed within 5 min of depressurizing the pressure vessel.

The foamed samples are analyzed in several ways. Bulk foam density ($\rho_f$) is determined via water displacement. The amount of water displaced when submerging a sample in a small-diameter graduated cylinder and the weight of the sample determine its density. It is assumed that the foam is a predominantly closed-cell foam, and no water is absorbed by the sample. Cell concentration is calculated from scanning electron micrographs (JEOL FEG-SEM 6500). Foamed samples are frozen in liquid nitrogen, fractured, and sputter-coated with a thin layer (100 Å) of platinum. An accelerating voltage of 5 kV at a working distance of 15 mm is typically used. Images containing a minimum of 100 cells are then obtained at several magnifications. The number of cells per unit volume ($cm^3$) of original, unfoamed polymer is determined from[42]

$$N_0 = \left[\frac{nM^2}{A}\right]^{3/2}\left[\frac{1}{1 - V_f}\right] \tag{6}$$

where $n$ is the number of cells in the micrograph, $M$ the magnification of the micrograph, $A$ the area of the micrograph, and $V_f$ the void fraction of the foamed sample. The void fraction is defined as

$$V_f = 1 - \frac{\rho_f}{\rho} \tag{7}$$

where $\rho$ is the density of the unfoamed material (1.04 g/$cm^3$). $N_0$ therefore is the number of cells nucleated per $cm^3$ of polymer before the foaming began, assuming no coalescence occurred. The average cell size and size distribution are calculated using the aid of a software program (ImageTool, University of Texas Health Science Center). The same digital images used to estimate the cell concentration were loaded in the software, and the image scale bar was used to calibrate the software. The average diameter was determined by manually measuring the mean diameter of a minimum of 50 cells.

A particle size analyzer was used to further probe the size and distribution of particles in several of our blends. The particle size analyzer (Coulter LS230, Coulter Beckman Co.) uses Mie light scattering theory to determine size distributions of particles suspended in fluids. Details on the Mie theory and the LS230 can be found elsewhere.[43] The suspension fluid used for our materials was tetrahydrofuran (THF), which dissolves away the polystyrene matrix, leaving any insoluble matter suspended in THF.

**Reproducibility.** Processing conditions, such as temperature and pressure, can have a decided impact on the nucleation and growth of bubbles in the foaming process. Additionally, varying levels of small, solid contaminants can also act as nucleants.[44,45] During the course of this work, a significant variation in cell concentration was observed. In this section, we lay out processing and experimental conditions that reduce the effect of these variations on the interpretation of the results.

The melt blending, sample pressing procedure and foaming steps can all contribute to variations in the cell concentration. It is difficult to control the cleanliness in and around the batch mixer on the scale where nucleation effects are important. The presence of dust or other heterogeneous particles can drastically affect the nucleation rate. The mixer was manually cleaned, purged, and cleaned again to minimize impurities incorporated in the blend. The pressing procedure to create the circular samples can lead to residual stresses within the sample. Kweeder et al. theorize that microvoids created during a fast quench of polystyrene samples from the molten state can nucleate foam bubbles.[46] For the samples in this work, the cooling rate as described in the Experimental Section was kept constant, minimizing the differences in residual stresses between samples. The effect of variations in saturation pressure can also be significant. Especially at low pressures, the nucleation rate is a strong function of saturation pressure. At the saturation pressure of 3.5 MPa (500 psi) typically used in this paper, pressure fluctuations up to 0.35 MPa (50 psi) are expected as a result of the sensitivity of the pressure gauges. Variations in the cell concentration of less than 20% are expected due to the uncertainty in the saturation pressure.

Uncertainty also exists in the analysis of the digital images. To assess the error in using a single SEM image to estimate the cell concentration according to eq 6, nine SEM images were taken through the 2 mm thickness of one foamed polystyrene sample. The sample was saturated with carbon dioxide blowing agent at 3.5 MPa (500 psi) and foamed for 30 s at a temperature of 105 °C. The average cell concentration was $1.06 \times 10^{10}$ cells/$cm^3$ with a standard deviation of $\pm 0.21 \times 10^{10}$. Thus, our procedure of calculating the cell concentration from one micrograph gives 20% variability.

The effect of variations in the experimental conditions can be minimized through sound experimental design. Four separate polystyrene samples prepared with an identical processing history were foamed simultaneously. The cell concentration varied by no more than 20%. Carefully matching processing and foaming histories thus leads to consistent foaming performance. We recognize that the foaming procedure using this particular polystyrene intrinsically generates a high nucleation density. While we have no way of determining whether nucleation is homogeneous or heterogeneous or both, the base nucleation level is consistent and will be referred to as the homogeneous nucleation level throughout this paper. This is plausible since it is now recognized that homogeneous nucleation in foams takes place at much lower levels of supersaturation than was previously believed.[47]

For each series of additives reported in this paper, a polystyrene control sample with identical processing history was added to the pressure vessel. The effect of an additive on the cell concentration is then described with the following ratio:

$$\text{nucleation ratio: } N^*/N_0 \tag{8}$$

where $N^*$ is the nucleation density of the sample containing additive and $N_0$ is the nucleation density of the unmodified PS685D control sample. Wherever possible, the nucleation ratio is taken as the average of three independent foaming experiments for that particular blend.

## Results

**Polystyrene Homopolymer and Solid Nucleating Agents.** Polystyrene disks were pressurized to 3.5 MPa at 25 °C and absorbed an average of 6.5% carbon dioxide by weight after complete saturation. Immediately following depressurization, samples were foamed for 15, 30, 60, and 120 s at 105 °C and quenched in ice water. Figure 1 shows SEM micrographs of the resulting foams. The cell concentration, calculated using eq 6, is close to $10^{10}$ cells/$cm^3$ for all four samples, independent

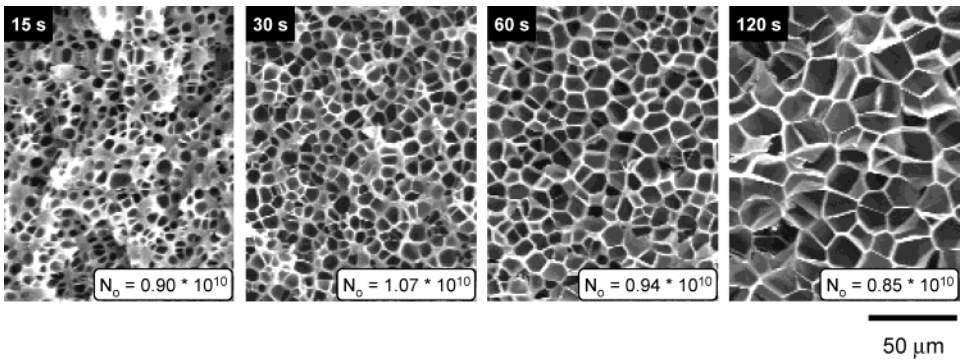


**Figure 1.** SEM micrographs of PS 685D samples foamed for 15−120 s at 105 °C. The nearly constant cell density indicates negligible coalescence during the experimental time frame.

**Table 1. Physical Properties of Polystyrene Foams at Various Foaming Times**

| foam time (s) | bulk density (g/cm$^3$) | cell diameter (μm) | cell density ($10^{10}$ cells/cm$^3$) |
|---|---|---|---|
| 15 | 0.47 | 5 | 0.90 |
| 30 | 0.33 | 9 | 1.07 |
| 60 | 0.21 | 12 | 0.94 |
| 120 | 0.06 | 19 | 0.85 |

of foaming time. This suggests that no coalescence of growing cells occurs during the experimental time frame. But bulk foam density decreases and average cell diameter increases with increased foaming time due to cell growth (see Table 1).

Solid nucleating agents were melt-blended into the polystyrene matrix to check their impact on the nucleation mechanism. Talc and carbon black nucleants were added to the polystyrene at $^1/_2$ wt %. Using the particle size analyzer described above, the median particle size was 0.8 μm for talc and 0.6 μm for carbon black. Assuming uniformly distributed spherical particles with the above diameters, an estimate of the number of available nucleation sites can be obtained as

$$\frac{\text{nuclei}}{\text{cm}^3} = \frac{x_{\text{add}}}{\rho_{\text{add}}} \frac{\rho_{\text{blend}}}{V_{\text{p}}} \tag{9}$$

where $x_{\text{add}}$ is the weight fraction of additive, $\rho_{\text{add}}$ and $\rho_{\text{blend}}$ are the density of the additive and the blend, and $V_{\text{p}}$ is the volume of one particle. Using eq 9, the maximum number of potential nucleation sites is $0.7 \times 10^{10}$ per cm$^3$ for talc and $1.8 \times 10^{10}$ per cm$^3$ for carbon black, potentially providing a modest improvement over the nucleation in pure polystyrene.

Figure 2 shows the effect on nucleation due to the additives. A drop in cell concentration of over 2 orders of magnitude is seen with the carbon black additive, while adding talc did not affect the cell concentration significantly. The cell size distribution is heterogeneous for the samples containing talc, while it is more homogeneous for the samples containing carbon black. None of the samples tested here showed an increase in the cell concentration over the pure polystyrene material. For both additives, the actual number of cells in the final foam is significantly lower than the number of nuclei estimated from eq 9. Figure 3 shows the particle size distribution in blends containing 1% of talc and carbon black as determined via the particle size analyzer. The blend containing carbon black shows a large peak around 0.7 μm, close to its median size of 0.6 μm, but a few larger aggregates around 2−3 μm are also present. Samples containing talc show a small peak around 0.3 μm, but also a large peak around 2 μm, and a significant presence of particles up to 10 μm diameter. Increasing the intensity of mixing in the batch mixer to 150 rpm for up to 15 min provided no significant improvement in the final cell size and distribution for a select number of samples containing talc. Talc and carbon black are poorly dispersed and thus are ineffective nucleants.

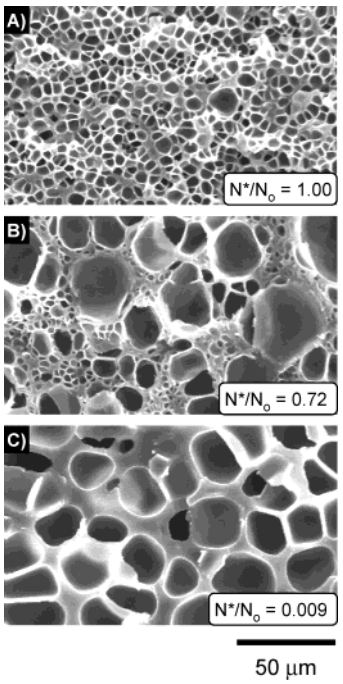


**Figure 2.** SEM micrographs of polystyrene foams containing talc and carbon black nucleating agents dispersed at 0.5 wt % and foamed for 30 s at 105 °C. Homopolymer polystyrene shows a uniform cell distribution (A). Talc leads to a highly polydisperse cell size distribution (B), while carbon black yields far fewer cells (C).

**Polystyrene-*block*-poly(ethylene propylene) Diblocks.** The first block copolymer tested as a nucleation site was a commercial Kraton PS-*b*-PEP diblock material. Kraton polymers and compounds are frequently used as processing additives to modify a variety of properties and are therefore appealing materials to consider here. Reedy and Rider[29] report on the use of styrene−ethylene/butylene−styrene block copolymer in a masterbatch formulation to be used in foam extrusion, yet no elaboration as to its specific role on the nucleation behavior is offered. In the current study, Kraton G1701, a diblock with a total molecular weight of 110 000 g/mol and PEP volume fraction of 0.67, is used.[48] The diblock was blended into PS 685D at $^1/_2$ and 2 wt % and

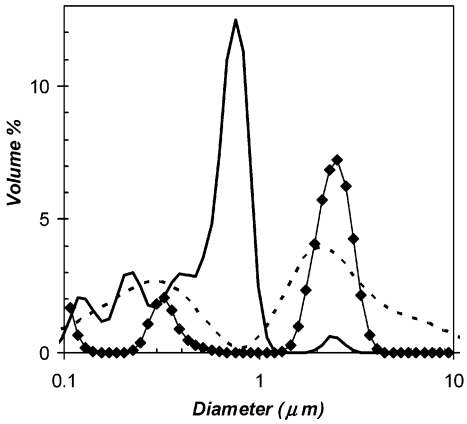


**Figure 3.** Particle size distribution detected for 1% of talc and carbon black in PS685D. The presence of larger aggregates around 2 $\mu$m in size are observed in blends containing carbon black (solid line) and talc (dashed line). The neat PS-*b*-PEP diblock also shows larger particles present with a 2 $\mu$m average size (◆).

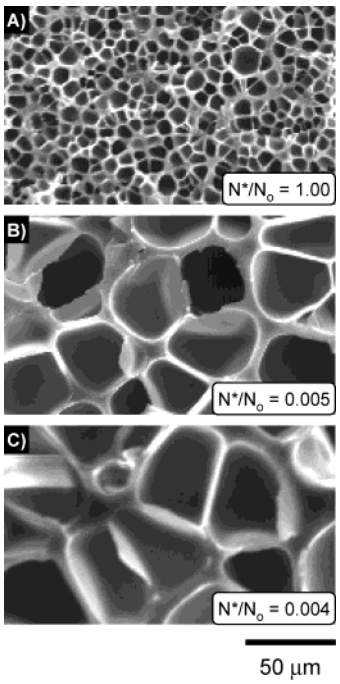


**Figure 4.** SEM micrographs of polystyrene foams with (A) 0.0, (B) 0.5, and (C) 2 wt % of a PS-*b*-PEP diblock added as a nucleating agent. The addition of this block copolymer leads to fewer large cells.

saturated with $CO_2$ at 3.5 MPa. Figure 4 shows SEM images of the foams obtained after 30 s of foaming at 105 °C. Foams containing the diblock material attained a much larger cell size. Significantly fewer cells are present, giving the much coarser structure observed. As was true for the homopolymer foams, Figure 5 shows a constant cell concentration as a function of foaming time, indicating that coalescence of growing bubbles is insignificant.

Confirmation of the existence of micelle sites was obtained by staining a sample containing 4 wt % of the PS-*b*-PEP diblock using ruthenium tetraoxide to provide contrast for TEM imaging. The TEM image in Figure 6A indicates potential micelle nucleants with an approximate radius of 50 nm exist in concentrations exceeding $10^{12}$ micelles/cm$^3$. Much larger structures with radii up to 300 nm, as shown in Figure 6B, are

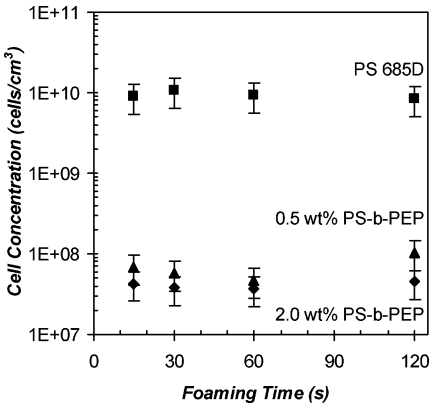


**Figure 5.** Cell concentration of polystyrene foams with various weight percentages of poly(styrene-*b*-ethyl propylene) diblock as a function of foaming time. Little coalescence is observed for any of the materials, but significantly fewer cells are present with the additive.

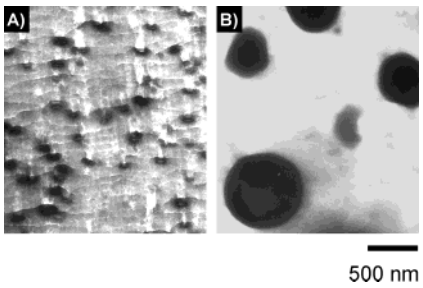


**Figure 6.** TEM images of a 4 wt % blend of PS-*b*-PEP in polystyrene 685D. (A) Micelles with a PEP core and an approximate radius of 50 nm. (B) Larger, nonequilibrium structures with a radius of up to 300 nm found in a different region of the same sample.

also observed in a different region of the same sample. These surfaces present a lower energy of activation for nucleation due to their increased radius of curvature. Particle size analysis with the light scattering method also indicates the large structures are present in the neat PS-*b*-PEP diblock. Figure 3 shows a peak in the PS-*b*-PEP diblock at 2.5 $\mu$m when dissolved in THF. It is not clear what this peak may represent, but filtering the dissolved PS-*b*-PEP material through a 0.2 $\mu$m filter and reprecipitating from THF before blending in the PS685D matrix had no effect on the nucleation behavior. This suggests the larger sites observed are nonequilibrium aggregates of block copolymer formed during the blending process, rather than an insoluble impurity. Regardless of their origin, the larger nucleation sites are more favorable and obscure any effect from the block copolymer micelles. A more uniformly distributed nucleant is needed for effective heterogeneous nucleation.

**Polystyrene-*block*-poly(methyl methacrylate) Diblocks.** The second diblock copolymer tested as a nucleation site was a well-characterized polymer synthesized in our laboratory. This polystyrene-*b*-poly(methyl methacrylate) (PS-*b*-PMMA) diblock copolymer consists of 80 kg/mol of styrene and 80 kg/mol of methyl methacrylate for a total molecular weight of 160 kg/mol. The diblock was blended into the PS 685D homopolymer at 0.5 and 2.0 wt %. The resulting blend was saturated with $CO_2$ at 3.5 MPa and foamed for 30 s at 105 °C. Carbon dioxide solubility is larger in the methacrylate block than in the ethylene−propylene hydrocarbon block considered above. The solubility of carbon dioxide in various polymers is shown in Figure 7 at temperatures

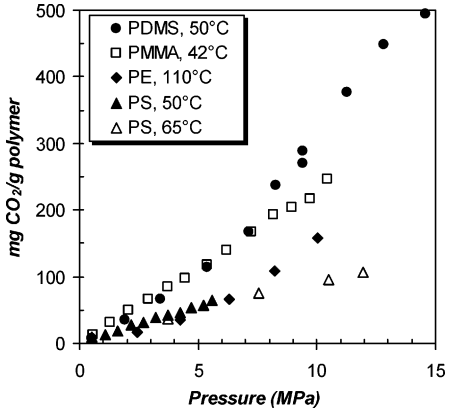


**Figure 7.** Solubility of carbon dioxide in several homopolymers.[49−52] Carbon dioxide solubility is significantly larger in PDMS and PMMA than polystyrene.

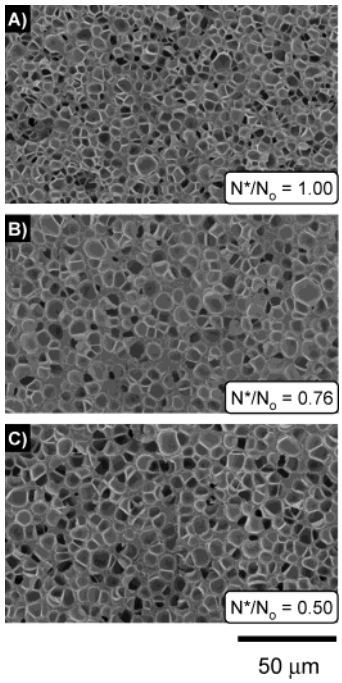


**Figure 8.** Cell concentration of blends containing (A) 0.0, (B) 0.5, and (C) 2.0 wt % of polystyrene-*b*-poly(methyl methacrylate) diblock copolymer. No significant change in cell size and number is observed.

near 50 °C.[49−52] Carbon dioxide is almost twice as soluble in PMMA than it is in PS or polyethylene (PE). This increased solubility near the micelle nucleants could lead to localized blowing agent concentration enhancement and increased probability of nucleation.

SEM images of the resulting foams are shown in Figure 8. The nucleated foam structure was significantly better for these blends than for the PS-*b*-PEP blends. Foams from blends with $^1/_2$ and 2 wt % of diblock nucleated an average of $4.8 \times 10^{10}$ and $3.0 \times 10^{10}$ cells/cm$^3$, respectively, similar to the average cell concentration in neat polystyrene foams. Cell size and distribution appear very uniform across these foams. A TEM image of the $^1/_2$ wt % blend is shown in Figure 9, showing uniformly dispersed micelles with an approximate radius of 30 nm. Assuming a nominal thickness of 50 nm for the TEM image, the concentration of micelles is estimated as $4.4 \times 10^{13}$ micelles/cm$^3$. In this estimate, we have divided the number of micelles observed per volume by a factor of 2, which accounts for double-counting micelles above and below the cutting plane. Equations 2 and 3 predict a micelle core with a radius of 18 nm and micelle concentrations of $9.3 \times 10^{13}$ for a 0.5 wt % blend. Both the theoretical calculation and visual image indicate a much higher number of potential nucleation sites than the observed cell concentration.

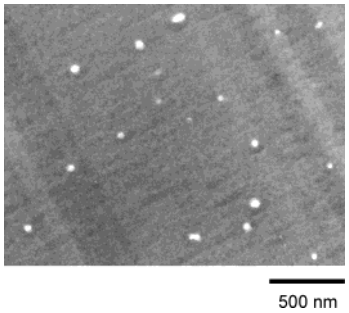


**Figure 9.** TEM image of a 0.5 wt % blend of PS-*b*-PMMA diblock in PS685D polystyrene. Uniformly distributed micelles of about 30 nm core radius are seen at a concentration of $4.4 \times 10^{13}$ micelles/cm$^3$.

**Silicone-Based Diblocks.** The final block copolymer tested as a nucleation site was a diblock containing a poly(dimethylsiloxane) block. Silicones and fluorine-containing polymers have been shown to have a high solubility in $CO_2$ at easily accessible temperatures and pressures.[53] Figure 7 shows that PDMS can take up more than twice as much $CO_2$ than PS at a pressure of 3.5 MPa. Two different PS-*b*-PDMS diblocks were blended into the polystyrene matrix at various concentrations. SD40 has a total molecular weight of 40 kg/mol, while SD156 has a total molecular weight of 156 kg/mol. Each diblock is symmetrical in polystyrene and poly(dimethylsiloxane) content, but the higher molecular weight diblock (SD156) forms larger micelles. Equations 2 and 3 predict a core radius of 16 nm and micelle concentration of $2.5 \times 10^{14}$ for a 0.5 wt % SD40 blend and 40 nm and $1.6 \times 10^{13}$ micelles/cm$^3$ for a 0.5 wt % SD156 blend. These calculated values are comparable to the lamellar repeat distance of the neat diblock copolymers as reported by Maric and Macosko.[54] The lamellar repeat distance can give a good estimate of the radius of a micelle formed using the same material in a homopolymer polystyrene matrix. Using small-angle X-ray scattering (SAXS) experiments, they found the spacing between lamella to be 22 nm for SD40 and 55 nm for SD156.

Both diblocks were blended into polystyrene at weight concentrations ranging from 0.5 to 2%. SEM images of the foams obtained from these blends are shown in Figure 10. The foams show a distinct heterogeneity in cell size distribution. Larger cells, similar in size to the uniform cell size found in the neat polystyrene control samples, are present along with cells that are significantly smaller. This bimodal cell size distribution indicates the added diblock did act as a preferred nucleant. Total cell concentration increased for both of the PS-*b*-PDMS diblocks. The presence of the micelles positively influenced the nucleation density, but the final cell concentration is still well below what would be expected from the number of potential nucleation sites present.

## Discussion

Uniformly dispersed spherical micelle sites were formed in number concentrations larger than the cell

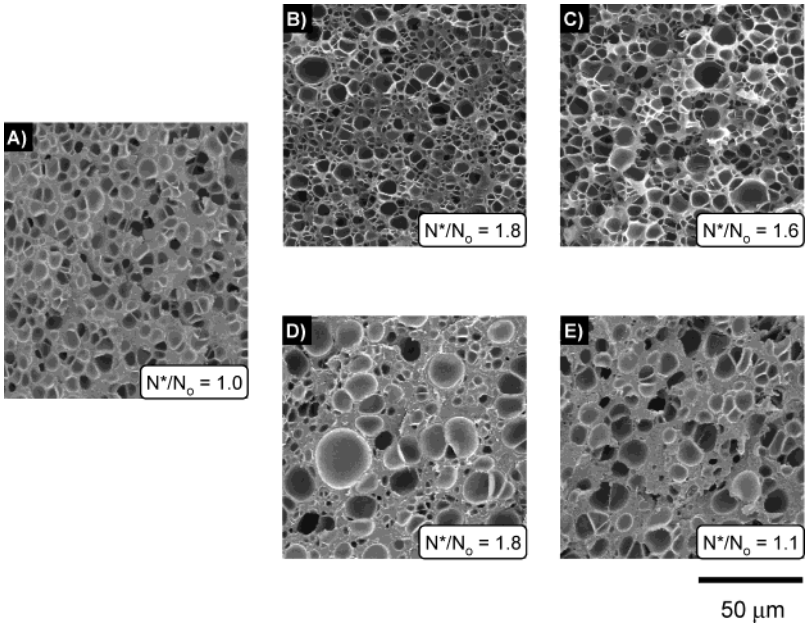


**Figure 10.** Cell concentration of foams from blends containing small weight percentages of polystyrene-*b*-poly(dimethylsiloxane) diblock copolymer compared to the neat polystyrene foam (A). With both 0.5 wt % (B) and 2.0 wt % (C) of the shorter SD40 diblock and 0.5 wt % (D) and 2.0 wt % (E) of the longer SD156 diblock, a modest increase in cell concentration is observed. There is also a distinct polydispersity in cell size with the addition of either diblock.

**Table 2. Summary of Additives and Effect on Foam Nucleation Density; Nucleation Density Reported after 30 s of Foaming at 105 °C**

| additive | $CO_2$[a] | $M_n$ (kg/mol) | $f_{PS}$ | core radius (nm) | wt % additive | $N^*$ ($10^{10}$ cells/cm$^3$) | $N^*/N_0$ |
|---|---|---|---|---|---|---|---|
| talc | | | | | 0.5 | 0.98 | 0.72 |
| carbon black | | | | | 0.5 | 0.029 | 0.009 |
| PS-*b*-PEP | 0.7[b] | 110 | 0.37 | 50[c] | 0.5 | 0.014 | 0.005 |
| | | | | | 2.0 | 0.012 | 0.004 |
| PS-*b*-PMMA | 2.0 | 160 | 0.5 | 18[d] | 0.5 | 4.8 | 0.8 |
| | | | | 30[c] | 2.0 | 3.0 | 0.5 |
| PS-*b*-PDMS | 1.7 | 40 | 0.49 | 16[d] | 0.5 | 6.1 | 1.8 |
| | | | | | 2.0 | 5.5 | 1.6 |
| | | 156 | 4.49 | 40[d] | 0.5 | 5.2 | 1.8 |
| | | | | | 2.0 | 2.7 | 1.1 |

[a] Relative solubility of $CO_2$ in block core compared to PS at 3.7 MPa and 50 °C. Also see Figure 7. [b] Estimate using $CO_2$ solubility in PE. [c] Estimated from TEM images. [d] Estimated using eq 2.

nucleation density observed in homopolystyrene foams. If these sites can act as ideal nucleants and effectively lower the minimum energy required to form a bubble, an increased nucleation rate would result. An almost 2-fold increase in cell concentration was observed for the PS-*b*-PDMS diblocks with a larger $CO_2$-philic micelle core, yet the cell concentration was still much lower than the number of potential sites present. None of the additives studied attained a final cell concentration on par with the number of potential nucleation sites present. In the case of the PS-*b*-PEP diblock, a significant *decrease* in cell concentration was actually observed. While micelles adhere to three of the four criteria for optimal nucleants, the energetics and/or kinetics of nucleation in/on the micelle are apparently not favorable. Table 2 summarizes the properties of the diblocks and the resulting foams.

When the amount of diblock additive is increased from 0.5 to 2%, Table 2 shows the number of cells present in the final foam decreased slightly for all blends. This indicates that the nucleation mechanism may not consist solely of heterogeneous nucleation at micelle nucleants. If this were so, an increase in the number of nucleants should increase the cell concentration. At 2 wt %, there may also be more aggregation of block copolymer than at 0.5 wt %.

The rheological behavior of the blend is one factor that could influence the nucleation and growth of cells. Changes in viscosity can influence both the nucleation and growth rates of bubbles. However, at the very small weight percentages of additives present in these studies, the rheological properties of the blends are not expected to change significantly. In both shear and extension, the differences in viscosity are small and considered to be within the reproducibility limits of these measurements.[55]

Heterogeneous nucleation is influenced by the type and size of the nucleation site. The work of formation for a nucleus on a flat, impermeable surface can be significantly lower than for homogeneous nucleation.[56] Fletcher found that nucleation on a strongly curved surface enjoys much less of this benefit.[31] As the radius of the nucleant decreases, approaching the size of the critical bubble nucleus, the reduction in the critical work of formation approaches the homogeneous limit. Similarly, as the contact angle $\theta$ approaches 180°, the reduction in the minimum work barrier decreases. Thus, surfaces with small radii of curvature and/or strong repulsive interactions (large contact angles) with the mixture are ineffective heterogeneous nucleation agents. Fletcher's work illustrates that there is a minimum effective nucleant size.

**Table 3. Surface Tensions of Polymers at the Foaming Temperature of 105 °C Calculated Using Eq 10[40]**

| polymer | $\sigma_0$ (mN/m) | $T_c$ (K) | $\sigma$ ($T$ = 378 K) (mN/m) |
|---|---|---|---|
| PS | 63.31 | 967 | 34.5 |
| PMMA | 65.09 | 935 | 34.5 |
| PDMS | 35.31 | 776 | 15.6 |
| PE | 56.38 | 921 | 29.6 |

All of the diblock systems listed in Table 2 form micelles with a radius close to the estimated critical radius of 20 nm, indicating their effectiveness as heterogeneous sites may be limited. However, the role of the micelles in the nucleation process is somewhat ambiguous. Unlike solid nucleants, nucleation could occur outside, on, or inside a block copolymer nucleant, i.e., on the corona of the micelle, at the A−B interface, or within the interior of the micelle. Nucleating on the corona of the micelle would not be energetically favored over homogeneous nucleation, as the corona consists of the same polymer as the matrix homopolymer. Nucleation on the A−B interface necessitates vacating part of the interface to be occupied by the nucleated bubble. This would require additional energy. Nucleation within the interior of the micelle seems most likely. The different properties of the B core block relative to the matrix material can provide a more favorable environment for nucleation to take place. In particular, a lower surface tension and higher blowing agent solubility in the core of the micelle would promote bubble nucleation inside the micelle. An ever thinning layer of block copolymers would then surround the growing bubble. This surface-active layer could reduce the surface energy of the nucleus. For this mechanism to be operative, a minimum nucleant size is required to provide sufficient diblock material to significantly reduce the surface energy of the critical nucleus.

Blends containing the PS-*b*-PDMS diblock copolymers were the only systems able to effectively increase the cell concentration of polystyrene foams. All three diblocks formed micelles similar in size, and both the PMMA and PDMS core blocks offered improved carbon dioxide solubility over the polystyrene matrix. PDMS is unique in that it offers the lowest surface tension. The work required to form a critical nucleus is proportional to the surface tension to the third power;[39] hence, small changes in surface tension can have a significant impact on the nucleation rate. The Guggenheim equation, originally developed for small-molecule liquids, has been found to describe the temperature dependence of surface tensions of polymer melts as well:[40]

$$\sigma = \sigma_0\left[1 - \frac{T}{T_c}\right]^{11/9} \tag{10}$$

where $\sigma_0$ is the surface tension at $T = 0$ K and $T_c$ is the critical temperature. Values for $\sigma_0$ and $T_c$ are obtained by least-squares regression of $\sigma$ vs $T$ and are readily available.[40] They are shown in Table 3 with the calculated surface tensions of PS, PMMA, and PDMS at the foaming temperature of 105 °C. The value for PE is also given for comparison. The surface tensions of PS and PMMA are identical, while the PDMS surface tension is significantly lower. Homogeneous nucleation within the PDMS core is thus favored over nucleation within the PS matrix. If nucleation were to happen at the interface, the lower PDMS surface tension would also translate into a smaller contact angle, again indicating a lowered work of formation and increased nucleation rate.

## Conclusions

We have investigated the use of spherical block copolymer micelles as novel nucleation sites in the formation of microcellular foams. Micelles are significantly smaller than solid nucleating agents and can be dispersed uniformly in high concentrations, making them promising nucleants. Using several different diblock copolymers added at low weight percentages to a polystyrene matrix, the nucleation behavior of the resulting blends was studied in a batch foaming process. None of the foams showed a large increase in cell concentration, as was originally anticipated from the number of potential nucleation sites present. We identify three key issues that may hinder the effectiveness of these block copolymer micelle nucleants. First, the size of the micelle is near the critical size of a nucleating bubble, which may be smaller than the minimum effective size. Second, aggregation of micelles (and solid nucleants) leads to a distribution of nucleation sites including a small number of larger, more favorable nucleation sites. This contributes to a heterogeneous cell size distribution in the foam. Finally, the high surface tension of most core components increases the work of formation and reduces the effectiveness of the micelles.

Blends containing micelles with a PDMS core component showed a bimodal cell size distribution and modest increase in cell concentration. The bimodal cell size distribution indicates a competition between multiple nucleation mechanisms. Thus, micelle nucleants appear to affect the cell nucleation mechanism in this system under these conditions. The batch foaming system used here intrinsically generates a large number of nuclei. This remarkably high cell concentration could be masking the effect of the block copolymer nucleants. Using a different polymer system with a lower carbon dioxide solubility could be helpful in isolating the effect of the block copolymer.

Several avenues for further study are identified from this work. Core components with lower surface tensions (such as PDMS), as well as larger micelles, will be better able to lower the work of formation and increase cell concentrations. Increasing the molecular weight of the block copolymer would increase the micelle size but typically also would make it harder to disperse and form monodisperse micelles. A micelle core containing a fluoropolymer would give a high affinity for $CO_2$ and also promote the formation of critical nuclei. Pursuing these avenues would further enhance our understanding of nucleation in polymeric foams.

**Acknowledgment.** The author thanks Milan Maric and Suping Lyu for donation of some of the block copolymers used in this study. Transmission electron micrograph images were contributed by Jennifer Dean and Kwanho Chang. This work was supported in part by the MRSEC Program of the National Science Foundation under Award DMR-9809364. R.B.M. received partial support for this work through a 3M nontenured faculty grant.

## References and Notes

(1) The Freedonia Group, Inc. *Foamed Plastics to 2005*; Study 1436: Cleveland, OH, 2001.

(2) Benning, C. J. *Plastic Foams; the Physics and Chemistry of Product Performance and Process Technology*; Wiley-Interscience: New York, 1969; Vol. 2.
(3) Klempner, D., Frisch, K. C., Eds. *Handbook of Polymeric Foams and Foam Technology*; Oxford University Press: New York, 1991.
(4) Zhang, H.; Rizvi, G. M.; Lin, W. S.; Guo, G.; Park, C. B. *SPE ANTEC Technol. Pap.* **2001**, 1746−1758.
(5) Suh, N. P. In *Innovation in Polymer Processing: Molding*; Stevenson, J. F., Ed.; Hanser: New York, 1996; p 97.
(6) Kumar, V. *Cell. Polym.* **1993**, *12*, 207−223.
(7) Seeler, K. A.; Kumar, V. *SPE ANTEC Technol. Pap.* **1992**, 1496−1501.
(8) Matuana, L. M.; Park, C. B.; Balatinecz, J. J. *Cell. Polym.* **1998**, *17*, 1−16.
(9) Collias, D. I.; Baird, D. G. *Polym. Eng. Sci.* **1995**, *35*, 1167−1177.
(10) Baldwin, D. F.; Suh, N. P. *SPE ANTEC Technol. Pap.* **1992**, 1503−1507.
(11) Shimbo, M.; Baldwin, D. F.; Suh, N. P. *Polym. Eng. Sci.* **1995**, *35*, 1387−1393.
(12) Jacobsen, K.; Pierick, D. *SPE ANTEC Technol. Pap.* **2000**, *58*, 1929−1933.
(13) Baldwin, D. F.; Park, C. B.; Suh, N. P. *Polym. Eng. Sci.* **1996**, *36*, 1425−1435.
(14) Hansen, R. H.; Martin, W. M. *Ind. Eng. Chem. Prod. Res. Dev.* **1964**, *3*, 137−141.
(15) Hansen, R. H.; Martin, W. M. *J. Polym. Sci., Part B: Polym. Lett.* **1965**, *3*, 325−330.
(16) Colton, J. S.; Suh, N. P. *Polym. Eng. Sci.* **1987**, *27*, 485−492.
(17) Colton, J. S.; Suh, N. P. *Polym. Eng. Sci.* **1987**, *27*, 493−499.
(18) Lee, S.-T. *Polym. Eng. Sci.* **1993**, *33*, 418−422.
(19) Lee, S.-T. *J. Cell. Plast.* **1994**, *30*, 444−453.
(20) Ramesh, N. S.; Rasmussen, D. H.; Campbell, G. A. *Polym. Eng. Sci.* **1994**, *34*, 1698−1706.
(21) Ramesh, N. S.; Rasmussen, D. H.; Campbell, G. A. *Polym. Eng. Sci.* **1994**, *34*, 1685−1697.
(22) Yang, H.-H.; Han, C. D. *J. Appl. Polym. Sci.* **1984**, *29*, 4465−4470.
(23) Rodrigue, D.; Woelfle, C.; Daigneault, L. E. *Blowing Agents and Foaming Processes 2001;* ChemTec: Toronto, 2001; p 5.
(24) Park, C. B.; Cheung, L. K.; Song, S.-W. *Cell. Polym.* **1998**, *17*, 221−251.
(25) Chen, L.; Blizard, K.; Straff, R.; Wang, X. *J. Cell. Plast.* **2002**, *38*, 139−148.
(26) McClurg, R. B. *Chem. Eng. Sci.*, in press.
(27) Walther, B. W. U.S. Patent 5,905,097, 1999.
(28) Gluck, G.; Hahn, K.; Henn, R.; Wassmer, K.-h.; Gausepohl, H.; Knoll, K.; Batscheider, K.-h., U.S. Patent 5,880,166, 1999.
(29) Reedy, M. E.; Rider, E. W. J. U.S. Patent 5,218,006, 1993.
(30) Cole, R. *Adv. Heat Transfer* **1974**, *10*, 85.
(31) Fletcher, N. H. *J. Chem. Phys.* **1958**, *29*, 572.
(32) Mayes, A. M.; Olvera de la Cruz, M. *Macromolecules* **1988**, *21*, 2543−2547.
(33) Kinning, D. J.; Thomas, E. L.; Fetters, L. J. *Macromolecules* **1991**, *24*, 3893−3900.
(34) Matsen, M. W. *Macromolecules* **1995**, *28*, 5765−5773.
(35) Whitmore, M. D.; Smith, T. W. *Macromolecules* **1994**, *27*, 4673−4683.
(36) Brandrup, J., Immergut, E. H., Grulke, E. A., Eds.; *Polymer Handbook*, 4th ed.; Wiley: New York, 1998.
(37) Fetters, L. J.; Lohse, D. J.; Richter, D.; Witten, T. A.; Zirkel, A. *Macromolecules* **1994**, *27*, 4639−4647.
(38) Young, R. J.; Lovell, P. A. *Introduction to Polymers*, 2nd ed.; Chapman & Hall: London, 1991.
(39) Gibbs, J. W. *Scientific Papers*; Dover Publications: New York, 1961; Vol. 2.
(40) Wu, S. *Polymer Interface and Adhesion*; Marcel Dekker: New York, 1982.
(41) Martini-Vvedensky, J. E.; Suh, N. P.; Waldman, F. A. U.S. Patent 4,473,665, 1984.
(42) Kumar, V.; Suh, N. P. *Polym. Eng. Sci.* **1990**, *30*, 1323−1329.
(43) Xu, R.-L. In *Liquid- and Surface-Borne Particle Measurement Handbook*; Knapp, J. Z., Barber, T. A., Lieberman, A., Eds.; Marcel Dekker: New York, 1996.
(44) Throne, J. L. *Thermoplastic Foams*; Sherwood Publishers: Hinckley, 1996.
(45) Lee, S. T., Ed.; *Foam Extrusion: Principles and Practice*; Technomic: Lancaster, PA, 2000.
(46) Kweeder, J. A.; Ramesh, N. S.; Campbell, G. A.; Rasmussen, D. H. *SPE ANTEC Technol. Pap.* **1991**, 1398−1400.
(47) Lubetkin, S. D. *Langmuir* **2003**, *19*, 2575−2587.
(48) Liu, Z.; Pappacena, K.; Cerise, J.; Kim, J.; Durning, C. J.; O'Shaughnessy, B.; Levicky, R. *Nano Lett.* **2002**, *2*, 219−224.
(49) Hilic, S.; Boyer, S. A. E.; Padua, A. A. H.; Grolier, J. P. E. *J. Polym. Sci., Part B: Polym. Phys.* **2001**, *39*, 2063−2070.
(50) Wissinger, R. G.; Paulaitis, M. E. *J. Polym. Sci., Part B: Polym. Phys.* **1987**, *25*, 2497−2510.
(51) Garg, A.; Gulari, E.; Manke, C. W. *Macromolecules* **1994**, *27*, 5643−5653.
(52) Chaudhary, B. I.; Johns, A. I. *J. Cell. Plast.* **1998**, *34*, 312−328.
(53) Davidson, T. A.; Jones, T. A.; Canelas, D. A.; DeSimone, J. M. *ACS Polym. Prepr.* **1998**, *39*, 463−464.
(54) Maric, M.; Macosko, C. W. *J. Polym. Sci., Part B: Polym. Phys.* **2002**, *40*, 346−357.
(55) Spitael, P. Foaming Thermoplastics: Heterogeneous Bubble Nucleation and Extensional Rheology. Ph.D. Thesis, University of Minnesota, Minneapolis, 2003.
(56) Turnbull, D.; Vonnegut, B. *Ind. Eng. Chem.* **1952**, *44*, 1292−1298.

MA049712Q